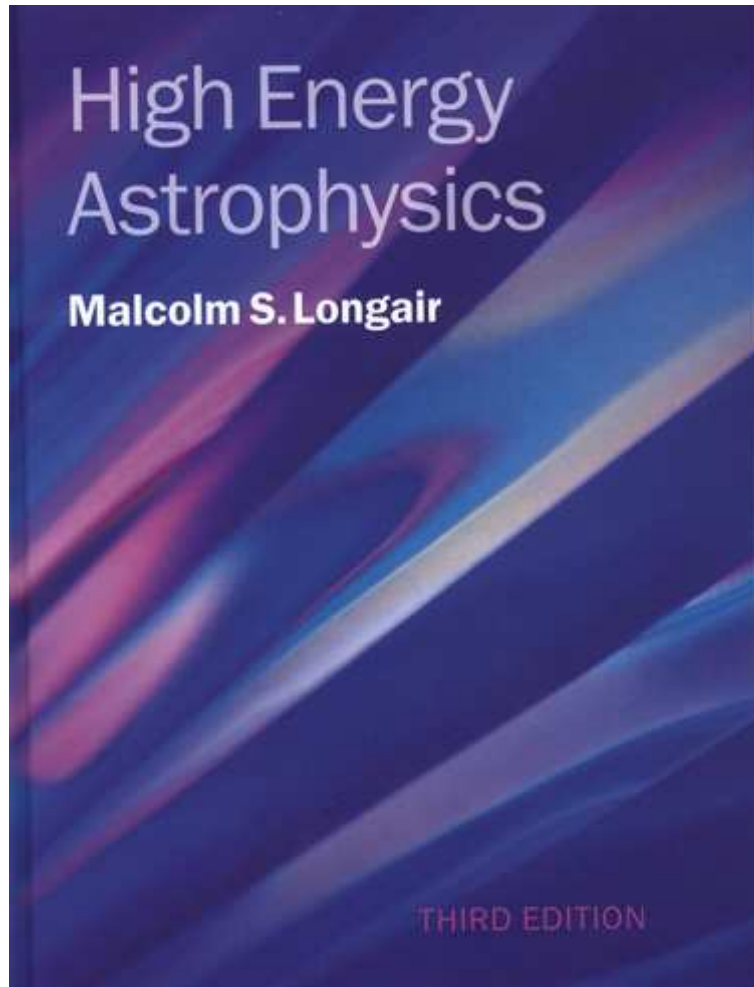
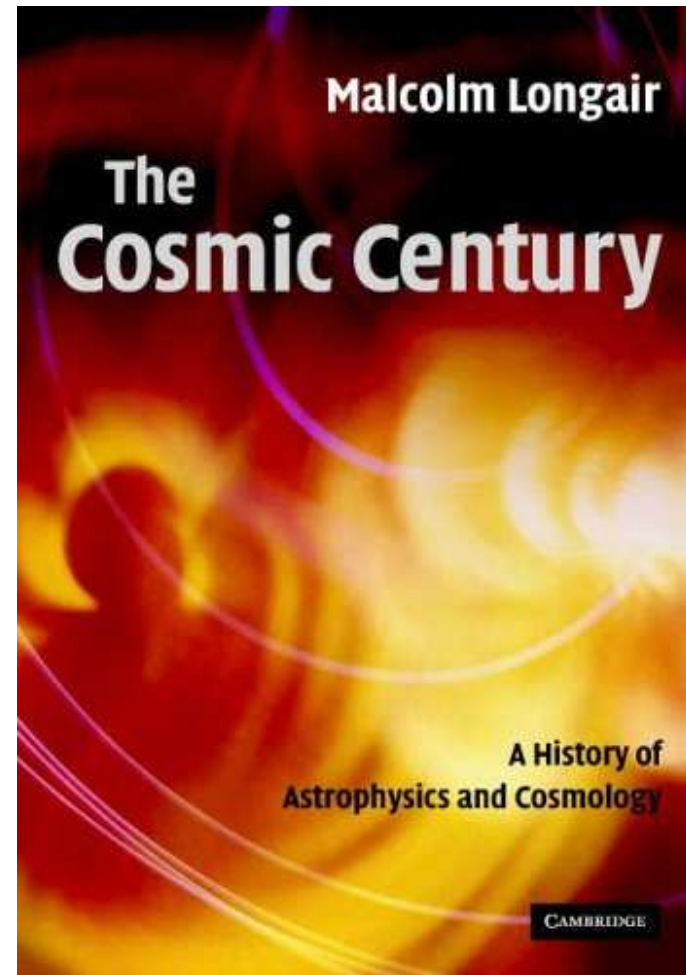


Introduction to High Energy Astrophysics

Books



2011

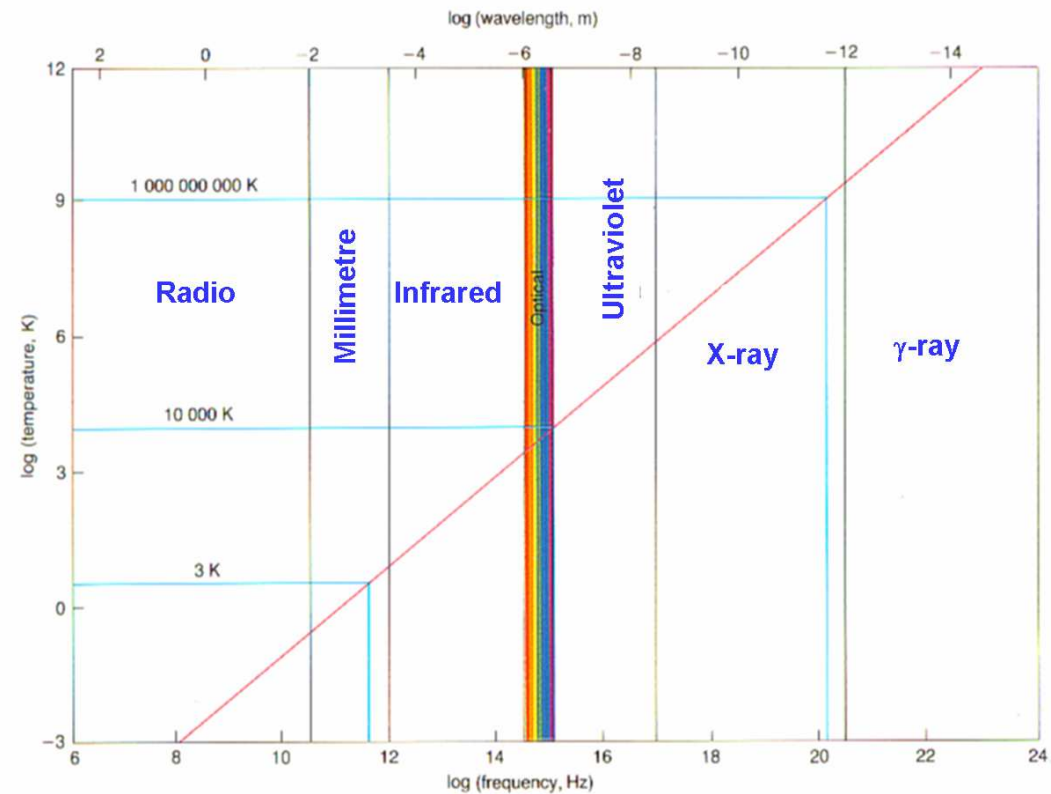


2006 - for the history of the subject

The Sky in Different Astronomical Wavebands

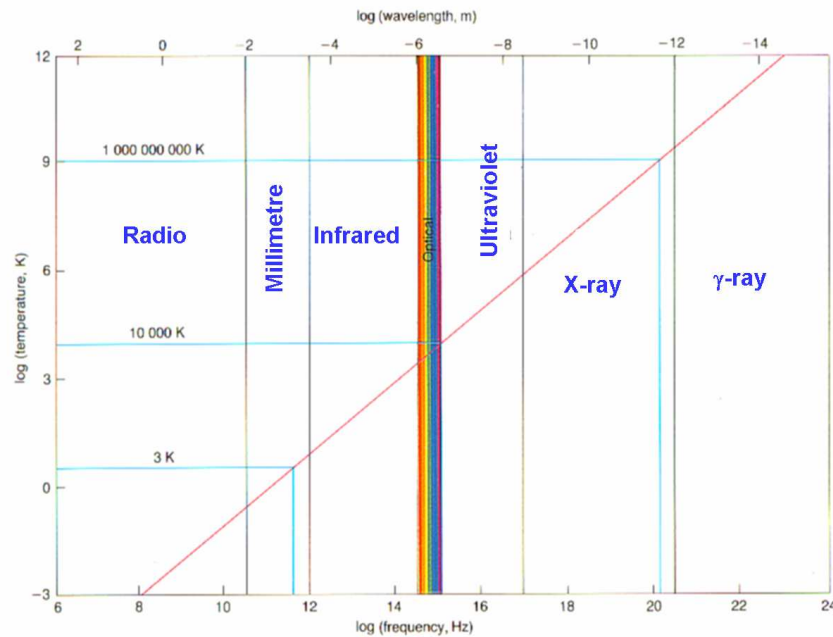
The context for high energy astrophysics

- Optical
- Infrared
- Millimetre-submillimetre
- Radio
- Ultraviolet
- X-ray
- γ -ray



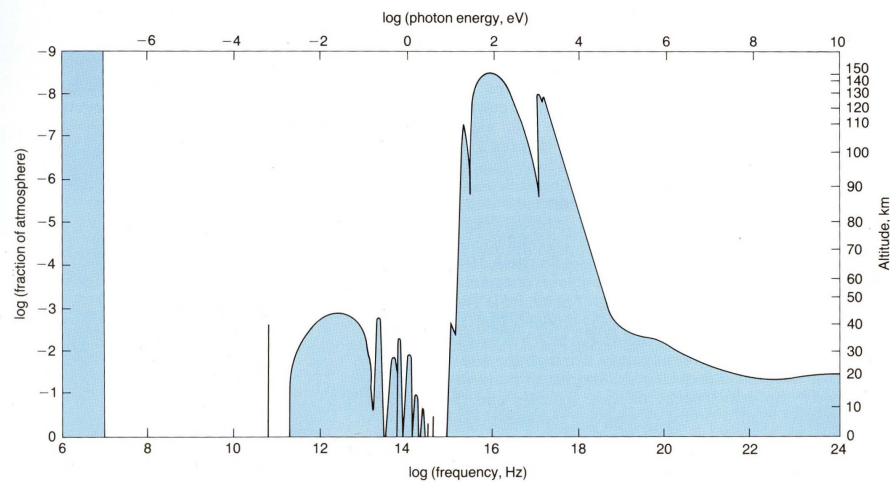
For blackbody radiation, $\nu_{\max} = 10^{11} (T/\text{K})\text{Hz}$ or $\lambda_{\max}T = 3 \times 10^6 \text{nm K}$.

The Transparency of the Atmosphere

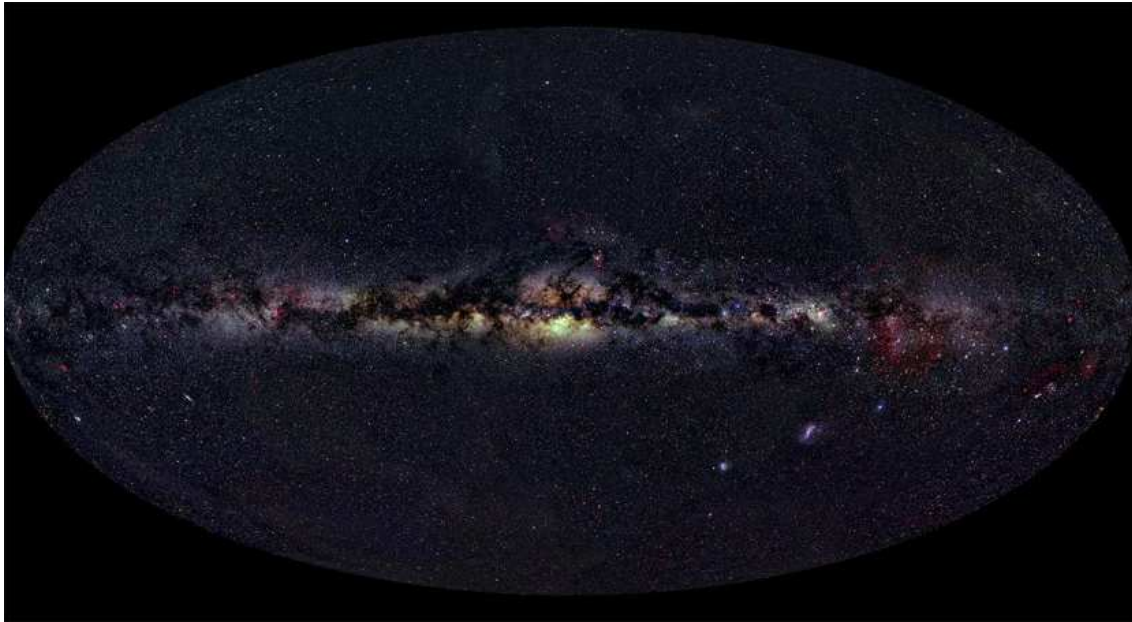


Until 1945, astronomy meant optical astronomy, corresponding to the wavelength range 300-800 nm, corresponding to temperatures of about 3000 - 10,000 K.

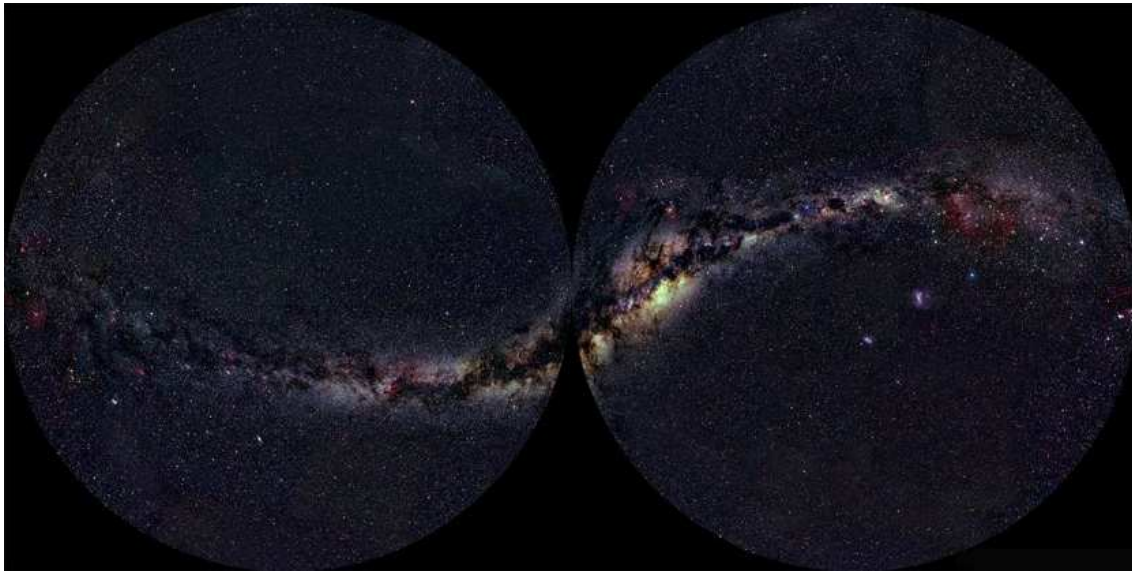
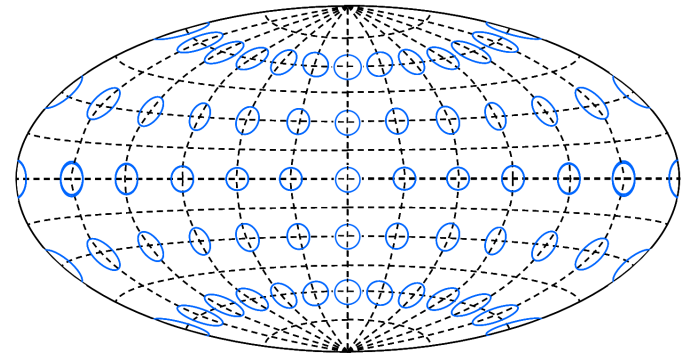
With the development of observational techniques for the other wavebands and the ability to place the telescopes above the atmosphere, the whole picture changed. High energy astrophysics was one of the major beneficiaries.



Optical Sky

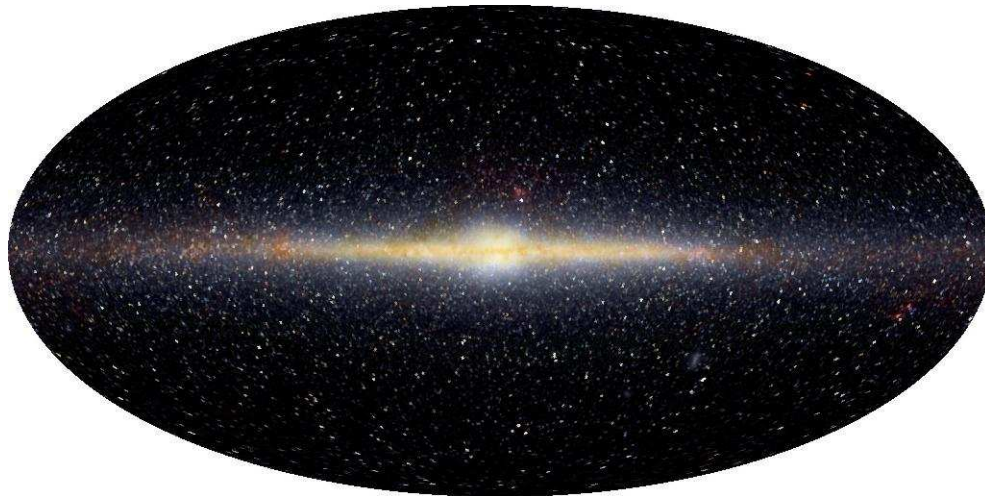


These images show the whole sky in different projections. The popular Hammer-Aitoff projection enables the whole sky to be depicted in a single image, but it is distorted.

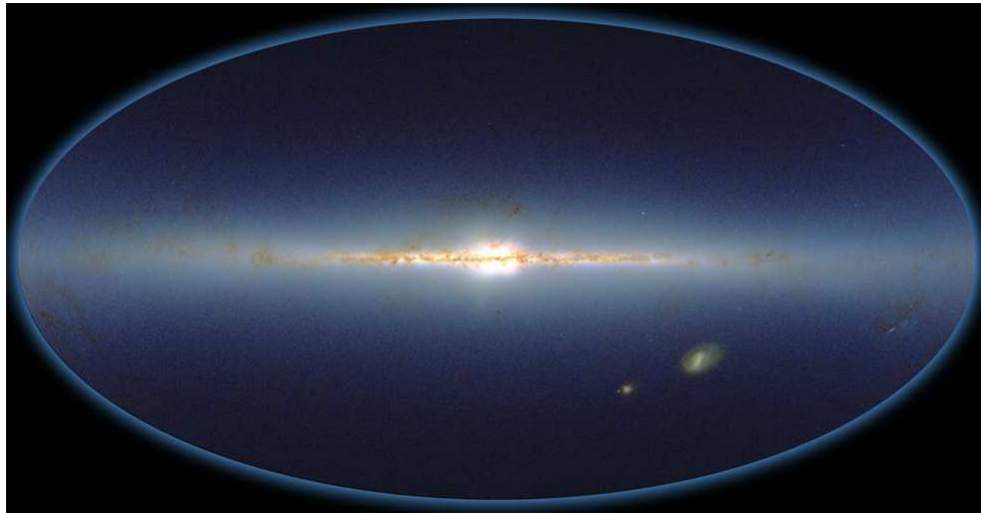


The image is dominated by the emission of **stars, ionised gas** and the **obscuring effect of interstellar dust**. In the Galactic Plane, typically one magnitude kpc^{-1} .

Infrared Sky

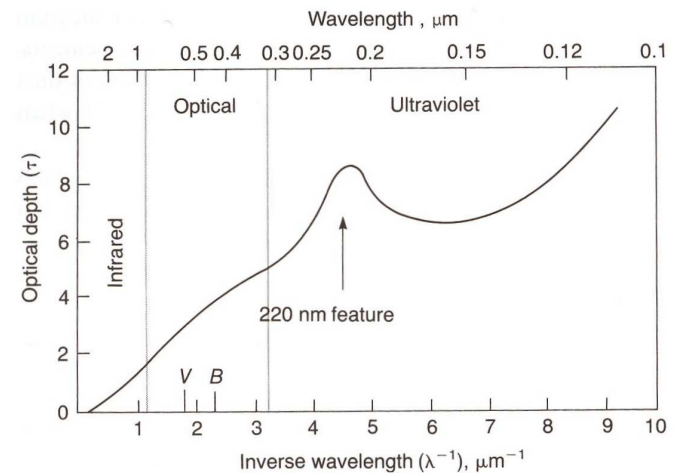


COBE



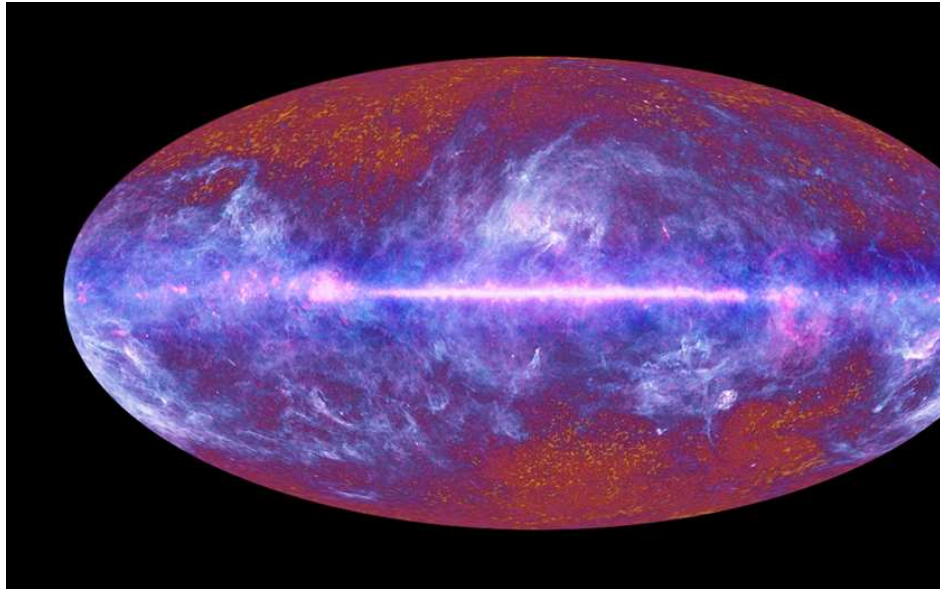
2MASS

The dust becomes transparent in the infrared waveband and so the distribution of thermal emission from the stars and hot gas clouds can be observed.



The extinction in astronomical magnitudes is shown relative to that at 900 nm.

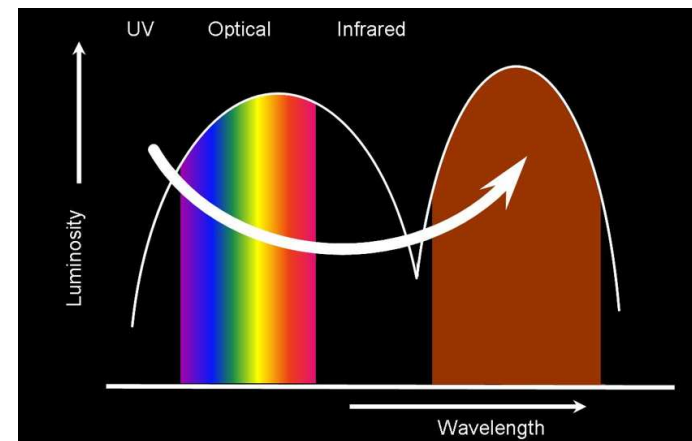
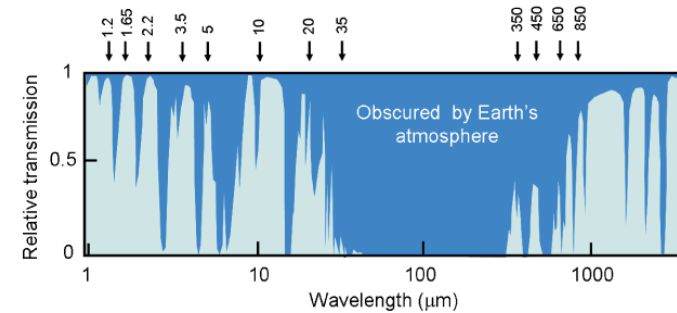
Far-infrared Sky



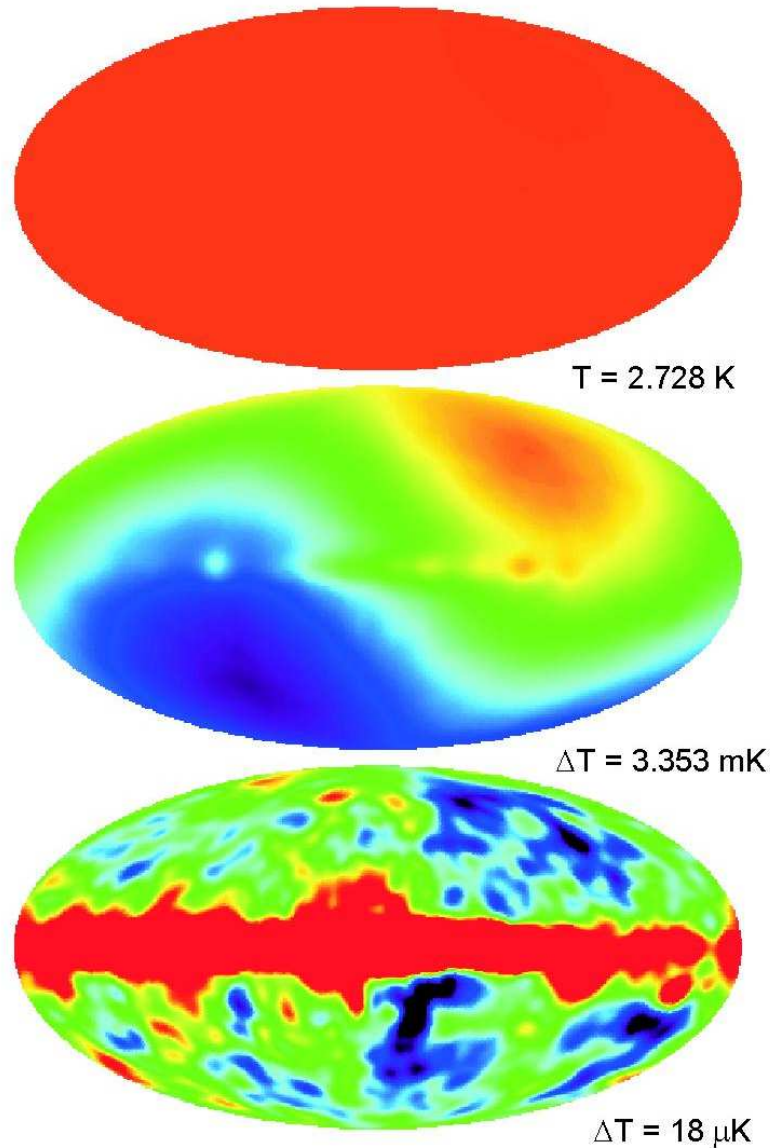
Planck

In addition, at the low temperatures of interstellar space, the dust becomes a strong emitter rather than an absorber of radiation. The dust acts as a transformer converting optical and ultraviolet photons into far infrared and submillimetre radiation.

The atmosphere becomes opaque in the far-infrared waveband and so the far-infrared waveband is best observed from space.



The Cosmic Microwave Background Radiation

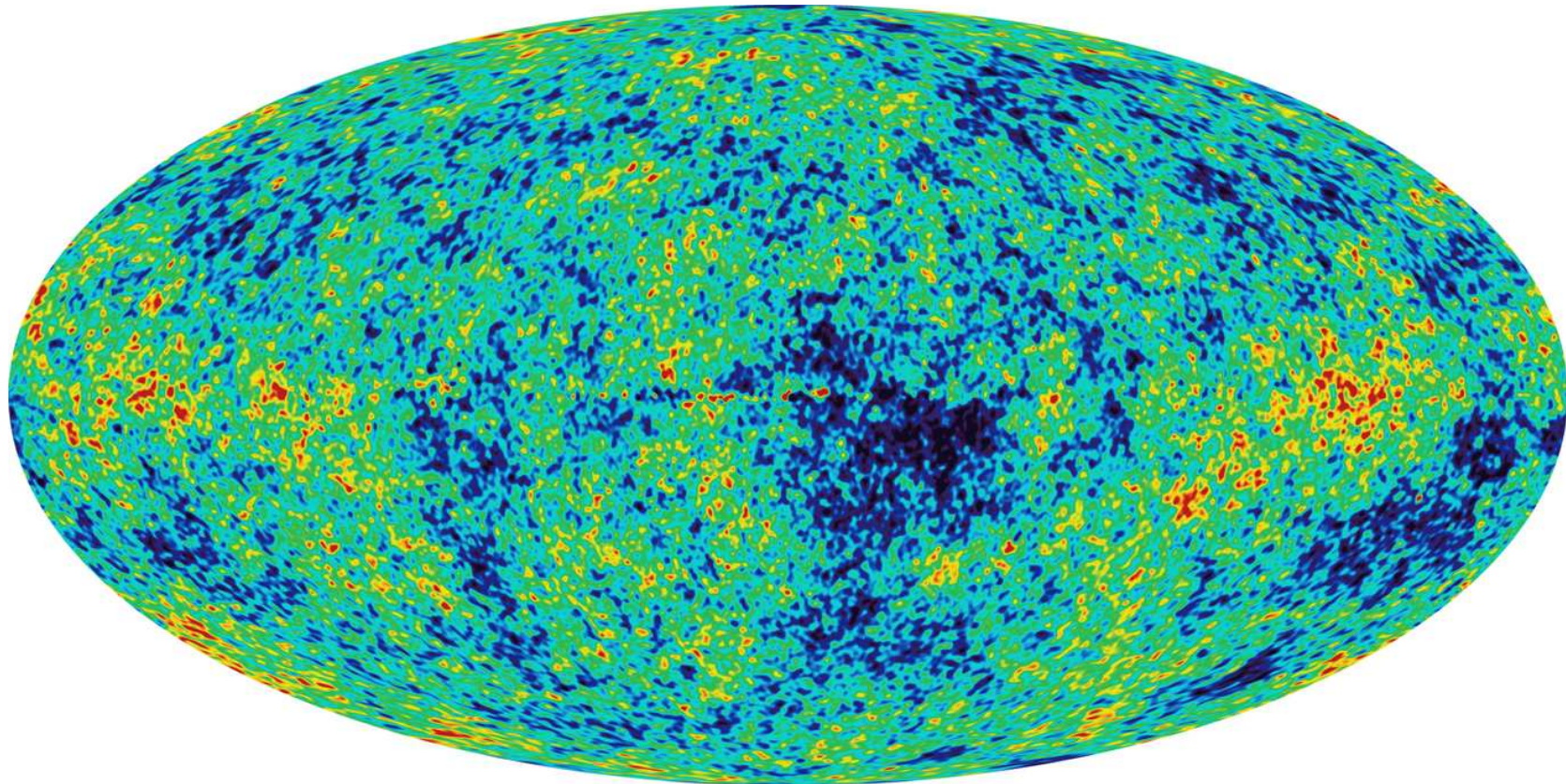


COBE

Maps of the whole sky at a wavelength of 5.7 mm (53 GHz) observed by the COBE satellite.

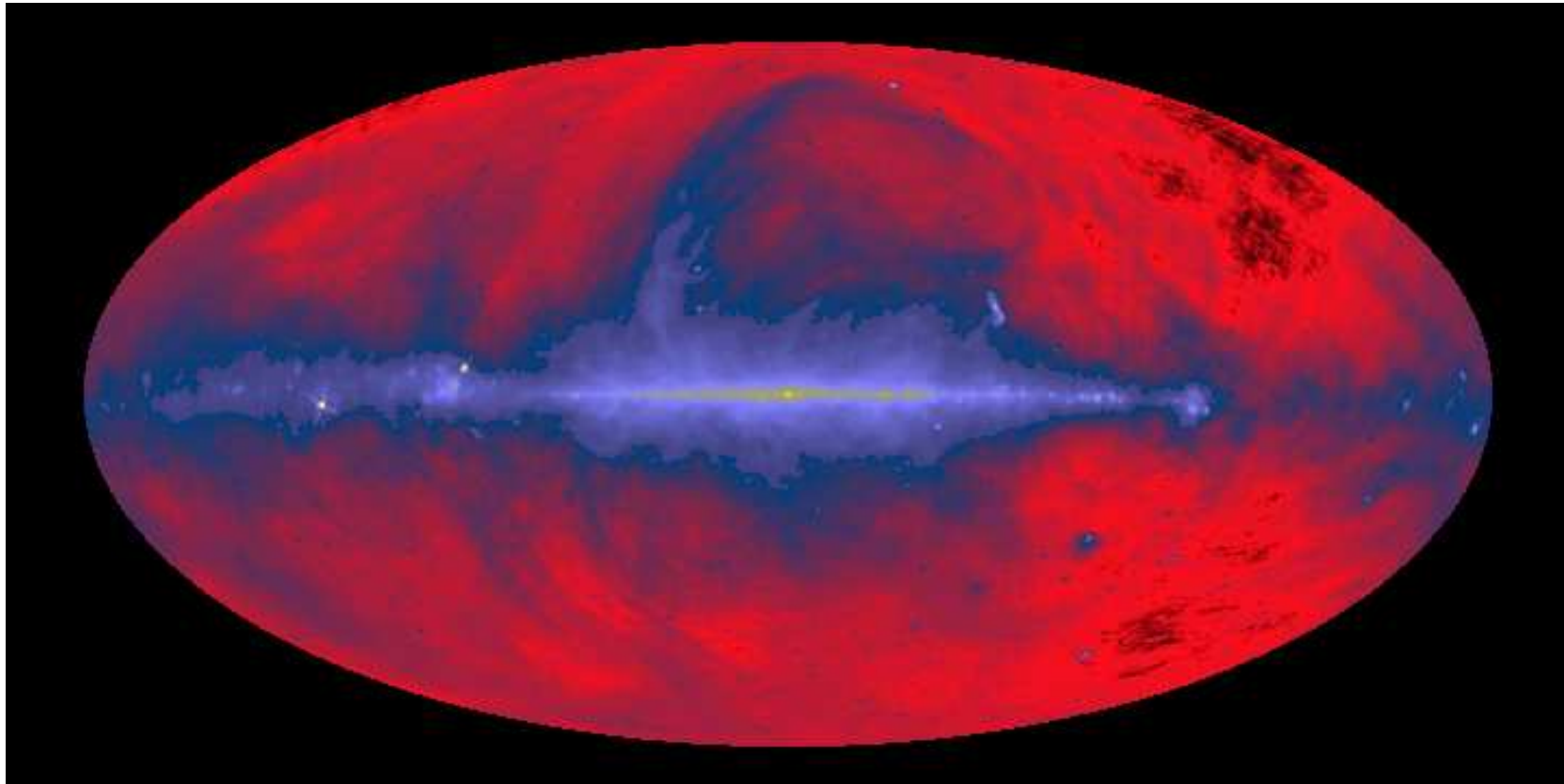
- The intensity over the whole sky.
- Once the uniform component is removed, the dipole component associated with the motion of the Earth through the isotropic reference frame is detected.
- Removing the dipole term reveals the cosmological fluctuations away from the Galactic plane.

The Cosmic Microwave Background Radiation



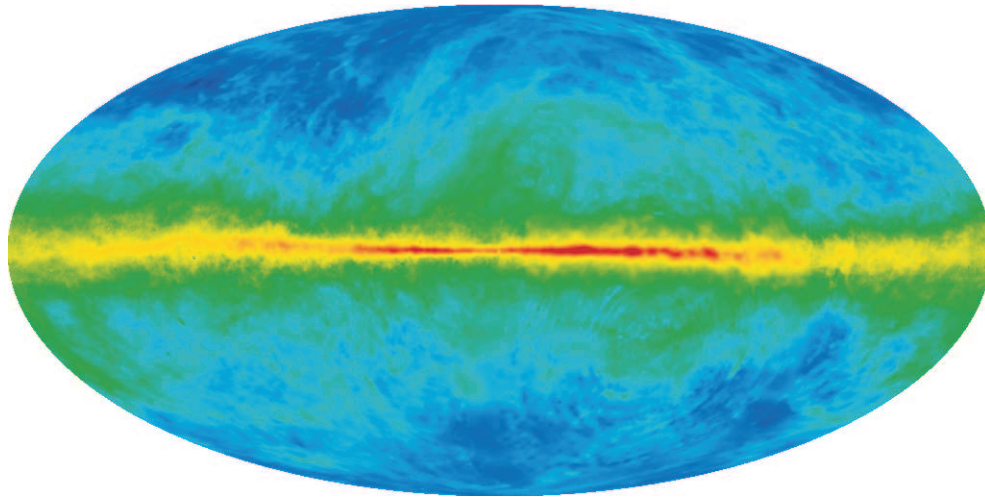
The superb observations of the Cosmic Background Radiation by the Wilkinson Microwave Anisotropy Probe have enabled a huge number of cosmological issues to be addressed observationally. The fluctuations are observed at a level of one part in 10^5 of the total intensity.

The Radio Background Emission

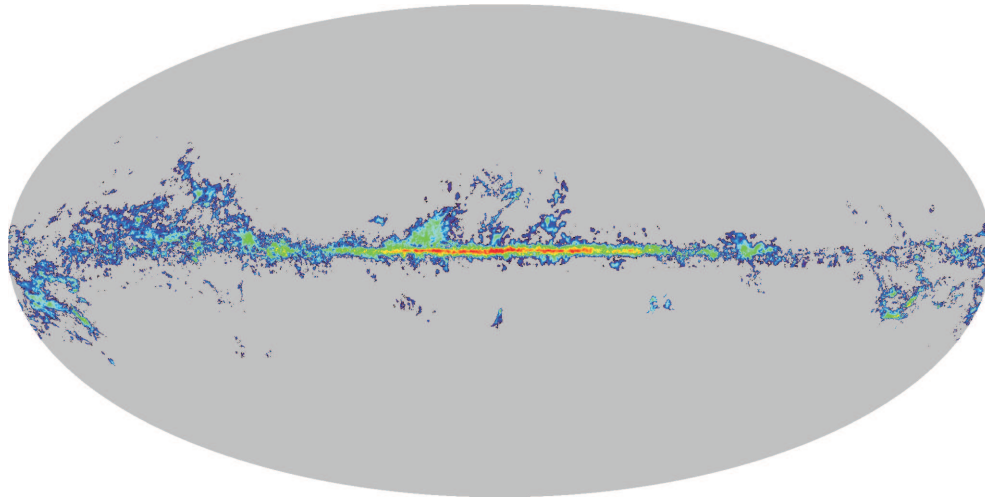


The radio emission of the Galaxy is the synchrotron radiation of ultrarelativistic electrons gyrating in the interstellar magnetic field. Note the giant loops of emission extending out of the Galactic plane.

The Neutral Hydrogen and CO Skies



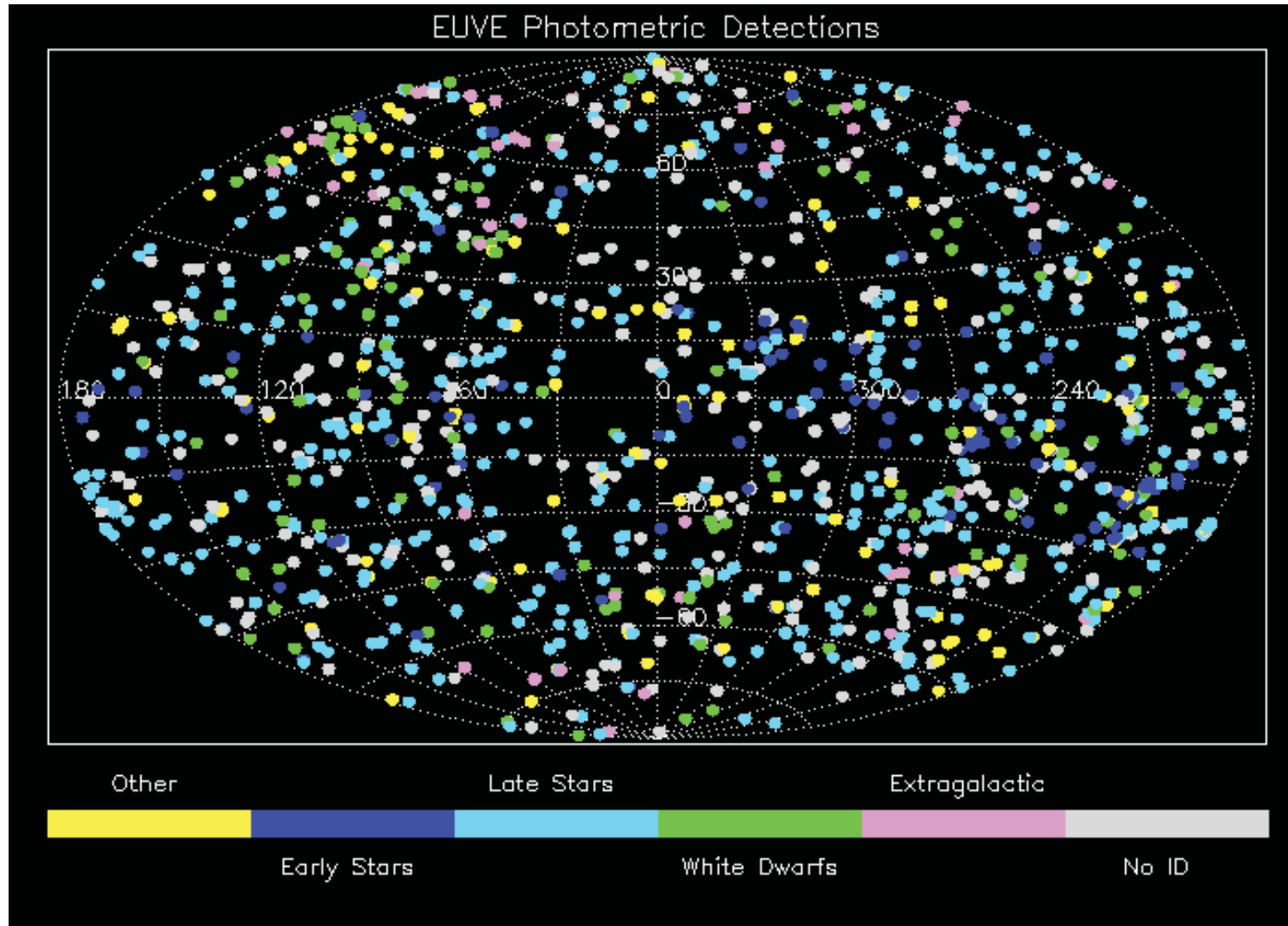
Neutral hydrogen image of the Galaxy



Carbon Monoxide map of the Galaxy

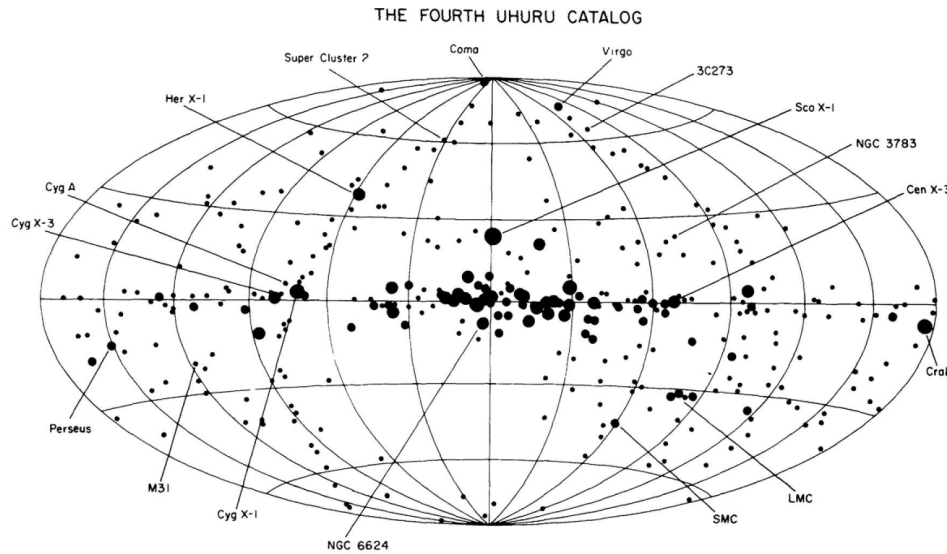
In contrast to the radio emission, the cold neutral hydrogen and carbon monoxide molecules are closely confined to the Galactic plane. The CO observations are a proxy for the distribution of molecular hydrogen which does not radiate by dipole radiation since it has no net dipole moment.

Ultraviolet Waveband

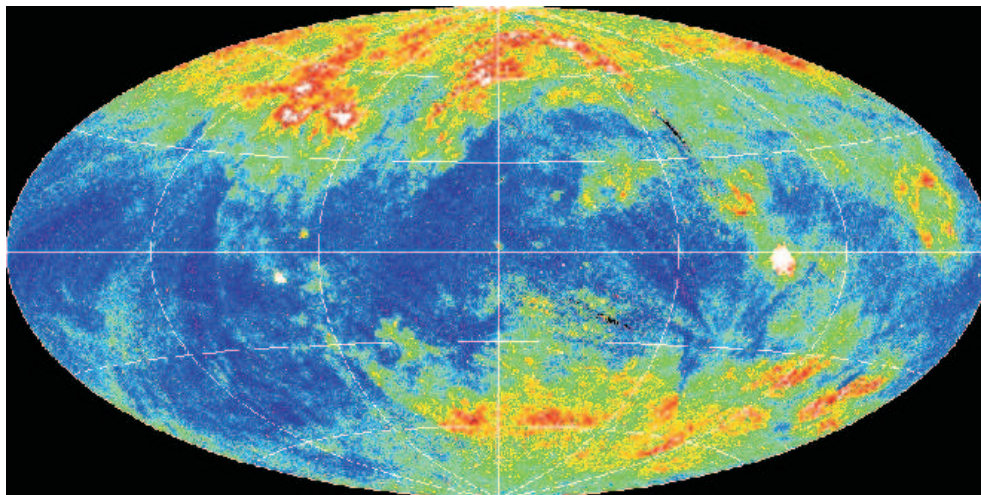


This image of the extreme ultraviolet waveband was made with the Extreme Ultraviolet Explorer (EUVE). Most of the 1200 objects are relatively nearby objects in our own Galaxy because of strong interstellar photoelectric absorption.

The X-ray Sky



X-ray sources in the 4th UHURU catalogue

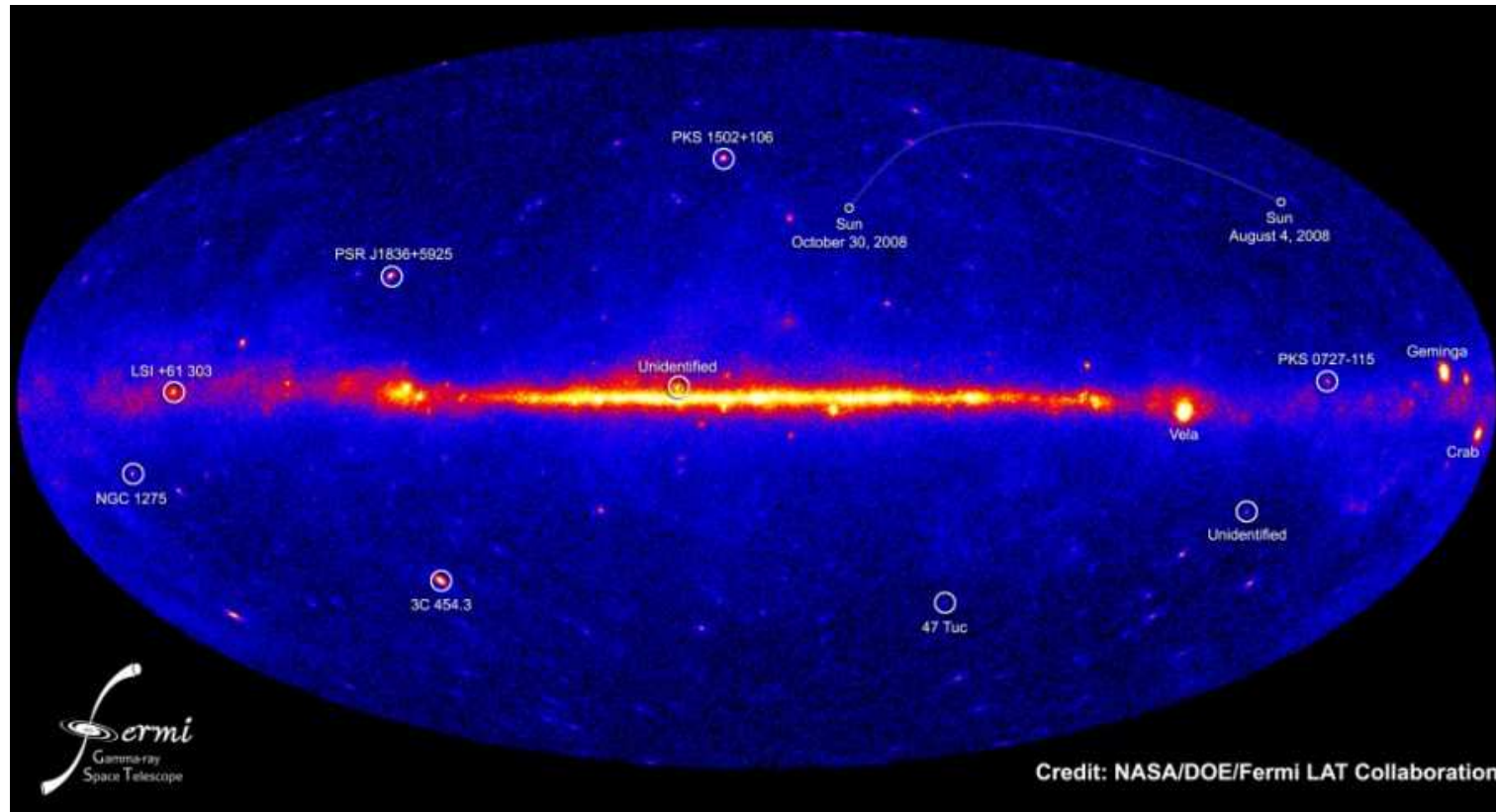


The diffuse low energy X-ray map of the sky.

The map of the brightest X-ray sources in the 2-6 keV waveband includes the quasar 3C273, the Perseus, Coma and Virgo clusters of galaxies, the radio galaxy Cygnus A, low and high mass X-ray binaries and supernova remnants.

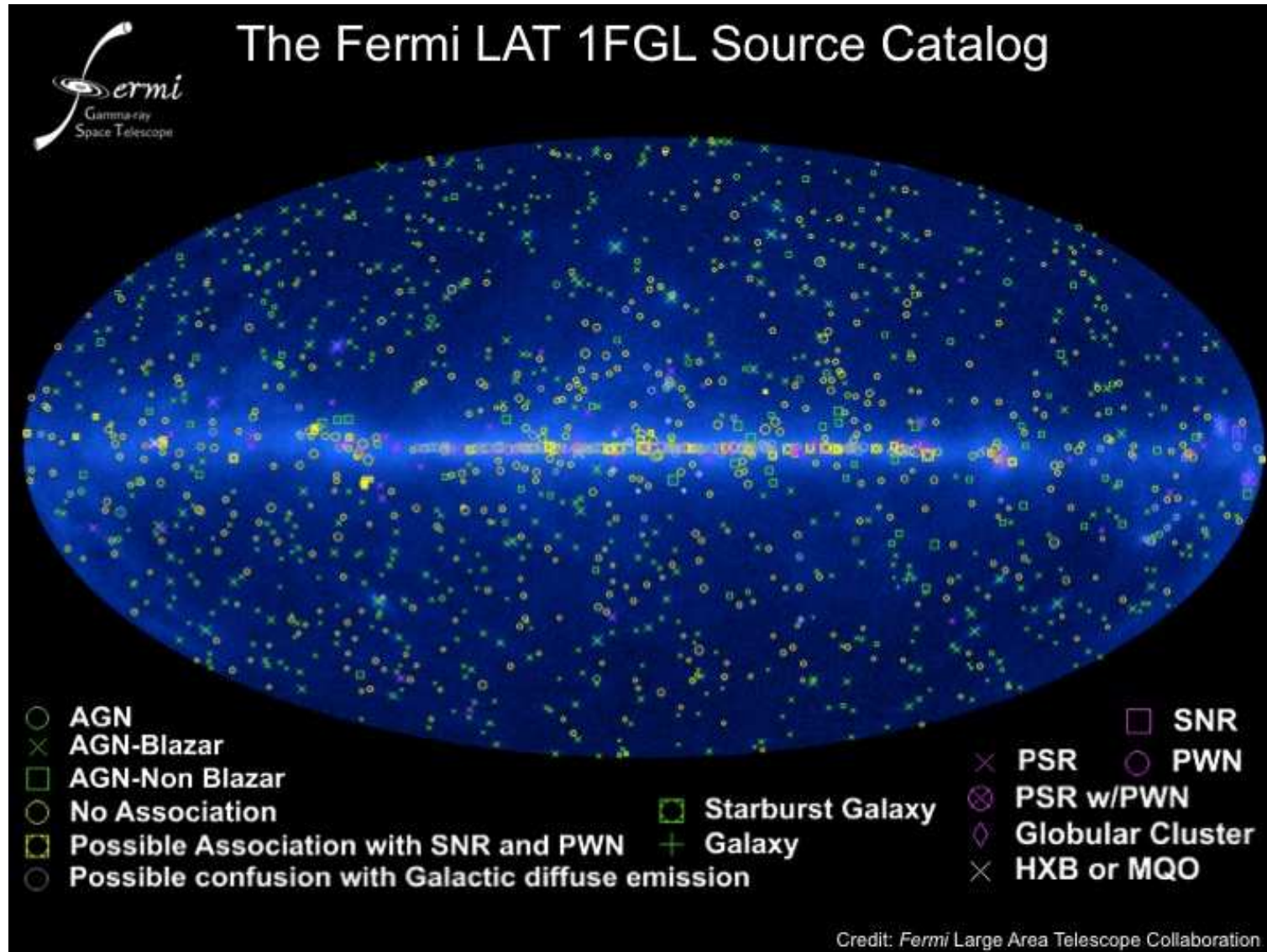
The image of the X-ray sky at 0.25 keV. The region close to the Galactic plane is less intense than at high latitudes because of interstellar X-ray absorption.

The γ -ray Sky

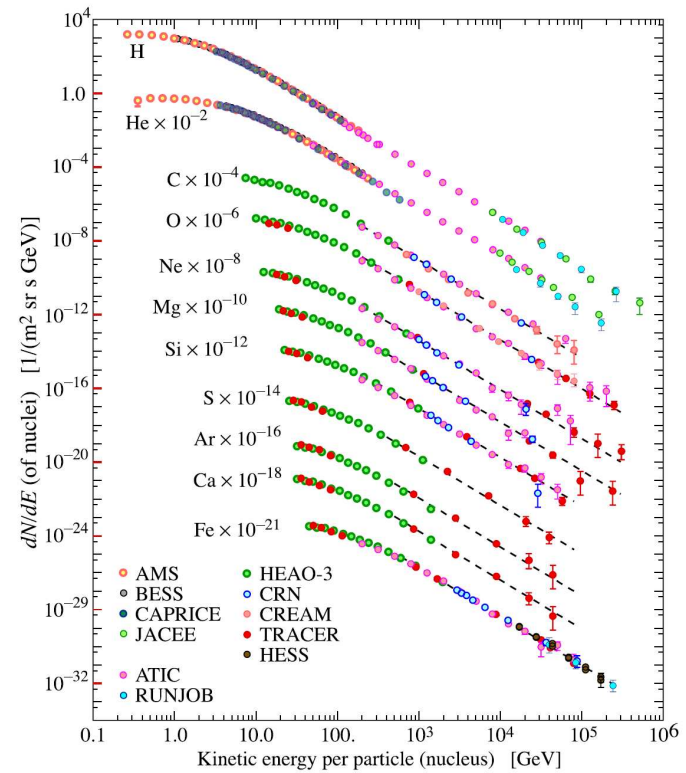
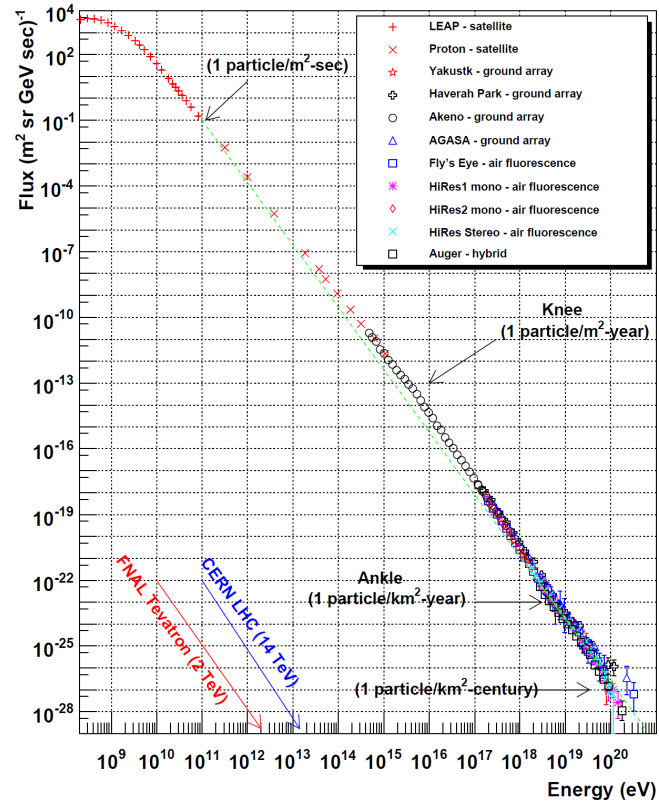


This image of the γ -ray sky was made by the Large Area Telescope of the Fermi Gamma-ray Space Telescope. The emission from the plane of the Galaxy is mostly π^0 decays. Away from the Galactic plane, most of the sources are associated with extreme active galactic nuclei and many exhibit superluminal motions in the associated radio sources.

Discrete sources in the γ -ray Sky



The Cosmic Rays



The intensity of primary nucleons in the energy range from several GeV to somewhat beyond 100 TeV is given approximately by

$$I_N(E) \approx 1.8 \times 10^4 E^{-x} \text{ nucleons m}^{-2} \text{ s}^{-1} \text{ sr}^{-1} \text{ GeV}^{-1}, \quad (1)$$

with $x = 2.7$ and E the energy per nucleon in GeV. There are however significant differences between the energy spectra of different elements.

High Energy Astrophysics

Basic astrophysical concepts

- White Dwarfs, Neutron Stars and Black Holes
- Accretion onto Compact Objects
- Accretion Discs
- The Masses of Black Holes in X-ray binaries and the Nuclei of Galaxies
- Clusters of Galaxies
- Jets

White Dwarfs, Neutron Stars and Black Holes

The most compact stars are *white dwarfs, neutron stars and black holes*. Their stability criteria can be found from the *virial theorem for degenerate stars*. For stellar material with a non-relativistic, non-degenerate equation of state, the condition for stability is given by the virial theorem in the form $3(\gamma - 1)U + \Omega = 0$, where U is the total internal thermal energy, γ is the ratio of specific heats of the stellar material and $\Omega = GM^2/R$ is the gravitational potential energy of the star. M is its mass and R is its mass and R a suitably chosen radius.

In the case of degenerate stars, the pressure is associated with the fact that fermions such as electrons, protons and neutrons cannot occupy the same quantum mechanical state. Simple arguments show that, in both the relativistic and non-relativistic cases, the pressure is independent of temperature:

$$\text{Non-relativistic : } p \approx \frac{\hbar^2}{m_e} \left(\frac{\rho}{m_p} \right)^{5/3}, \quad \text{Relativistic : } p \approx \hbar c \left(\frac{\rho}{m_p} \right)^{4/3}.$$

Inserting the non-relativistic formula into the equation of hydrostatic support enables solutions for low-mass white dwarfs and neutron stars to be found.

White Dwarfs, Neutron Stars and Black Holes

In the *relativistic case*, the total internal energy U is

$$U = V\varepsilon = 3Vp \approx V\hbar c \left(\frac{\rho}{m_p} \right)^{4/3}, \quad (2)$$

where ε is the energy density of the gas, which in the relativistic limit is related to the pressure by $p = \frac{1}{3}\varepsilon$. Therefore, the virial theorem becomes:

$$2U = |\Omega|, \quad 2V\hbar c \left(\frac{\rho}{m_p} \right)^{4/3} = \frac{1}{2} \frac{GM^2}{R}. \quad (3)$$

We can now approximate $V \approx R^3$ and $\rho V = M$. Therefore, (2) becomes

$$\frac{2\hbar c}{R} \left(\frac{M}{m_p} \right)^{4/3} = \frac{1}{2} \frac{GM^2}{R}. \quad (4)$$

This is the important result. Both the right and left-hand sides of the expression depend upon radius R in the same way. Dropping constants of order unity, the mass of the star is:

$$M \approx \frac{1}{m_p^2} \left(\frac{\hbar c}{G} \right)^{3/2} \approx 2M_\odot. \quad (5)$$

The Chandrasekhar Mass

This is the expression for the *Chandrasekhar mass* and is the upper limit for the mass of relativistic degenerate stars. If the mass were any greater, the gravitational term would always dominate and, since both the pressure and gravitational terms depend upon mass in the same way, the star would collapse indefinitely. The exact expression is

$$M_{\text{Ch}} = \frac{5.836}{\mu_e^2} M_{\odot}, \quad (6)$$

where $\mu_e m_u$ is the average particle mass per electron, which is 2 for a relativistic degenerate gas, except for hydrogen. A similar result applies for neutron stars, but the exact result is more difficult to work out since the effects of general relativity cannot be ignored.

The fine-structure constant is $\alpha = e^2/4\pi\epsilon_0\hbar c \approx 1/137$. The equivalent gravitational fine structure constant can be found by replacing $e^2/4\pi\epsilon_0$ by Gm_p^2 .

$$\alpha_G = \frac{Gm_p^2}{\hbar c} \approx 5.6 \times 10^{-39}, \quad (7)$$

reflecting the different strengths of the electrostatic and gravitational forces. Hence, the Chandrasekhar mass is $M \approx m_p \alpha_G^{-3/2}$. Stars are objects which possess about 10^{58} protons.

Black Holes

If the mass of the compact star is greater than about $2M_{\odot}$, it is inevitable that the object collapses to a *black hole*. It is convenient to consider separately the spherically symmetric, non-rotating black holes and those with non-zero angular momentum.

- **Schwarzschild Black Holes** are non-rotating and spherically symmetric. There is a surface of infinite redshift at the *Schwarzschild radius* R_g .

$$R_g = \frac{2GM}{c^2} = 3 \left(\frac{M}{M_{\odot}} \right) \text{ km.} \quad (8)$$

For an observer at infinity, radiation emitted at this radius is redshifted to zero frequency – this is why the black holes are called ‘black’. There is a last stable circular orbit about the black hole at radius $r = 3R_g$. If matter were placed on a circular orbit at radial distance less than $3R_g$, it would rapidly spiral into the black hole - this is why the black holes are called ‘holes’.

Black Holes

- **Kerr Black Holes** possess angular momentum J . The surface of infinite redshift occurs at radius

$$R_+ = \frac{GM}{c^2} + \left[\left(\frac{GM}{c^2} \right)^2 - \left(\frac{J}{Mc} \right)^2 \right]^{1/2}. \quad (9)$$

For a maximally rotating Kerr black hole, the term in square brackets is zero and then

$$R_+ = \frac{GM}{c^2}, \quad J_{\max} = \frac{GM^2}{c}. \quad (10)$$

The last stable circular orbit depends upon whether the test particle is corotating or counter-rotating with respect to the black hole:

$$\text{Corotating} \quad r = \frac{GM}{c^2} \quad : \quad \text{Counter-rotating} \quad r = \frac{9GM}{c^2}. \quad (11)$$

The corotating case in (10) is very important since it demonstrates that matter can approach much closer to $r = 0$ for a maximally rotating Kerr black hole than it can for a Schwarzschild black hole.

Accretion onto Compact Objects

Consider a mass m falling from infinity onto a compact mass M which has radius R . The kinetic energy of collapse is dissipated as heat when it hits the surface of the star.

$$\frac{GMm}{R} = \frac{1}{2}mv^2 = \text{Heat Dissipated.} \quad (12)$$

Suppose the matter is accreted at a rate \dot{m} . Then, the rate of dissipation of energy is

$$\frac{dE}{dt} = \frac{GM\dot{m}}{R}. \quad (13)$$

Expressing this result in terms of the *Schwarzschild radius*,

$$\frac{dE}{dt} = \frac{\dot{m}c^2}{2} \left(\frac{R_g}{R} \right). \quad (14)$$

For a neutron star of mass $1 M_\odot$, $R = 10$ km, according to this estimate, about 1/6 of the rest mass energy of the infalling matter is dissipated as heat. This is an overestimate since this calculation neglects the effects of general relativity which cannot be ignored in such compact objects.

Accretion onto Compact Objects

It is convenient to write the rate of energy generation, or the luminosity, of the source as

$$\frac{dE}{dt} = \eta \dot{m} c^2, \quad (15)$$

where η describes the efficiency of the accretion process. The following table shows the maximum efficiencies obtainable by various astrophysical processes.

<i>Form of energy production</i>	<i>η</i>
Chemical energy	10^{-9}
Nuclear energy	10^{-2}
Schwarzschild black holes	0.06
Kerr black holes	0.43
Rotational energy of black hole	0.29

- Thus, the accretion of matter onto rotating black holes is the most powerful energy source for objects such as X-ray binaries and active galactic nuclei.
- Black holes are the most compact objects which a mass M can have and so the shortest time-scale which can be associated with an object of mass M is $t \sim R_g/c \approx 10^{-5}(M/M_\odot)$ s.

The Eddington Luminosity

The amount of energy which can be obtained from accretion is not, however, unlimited. The maximum luminosity L is set by the balance between the attractive force of gravity acting on the protons and the repulsive force of radiation pressure acting on the electrons. In a fully ionised plasma, the protons and electrons are strongly coupled by electrostatic forces between protons and electrons:

$$f_{\text{grav}} = \frac{GMm_p}{r^2}, \quad f_{\text{rad}} = \sigma_T N_{\text{ph}} \frac{h\nu}{c},$$

where $N_{\text{ph}} = L/4\pi r^2 c$ is the flux density of photons at distance r from the source and σ_T is the Thomson cross-section. Thus, the attractive and repulsive forces both depend upon r^{-2} . Equating these forces, the *Eddington luminosity* L_E is

$$L_E = \frac{4\pi GMm_p c}{\sigma_T} = 1.3 \times 10^{31} \left(\frac{M}{M_\odot} \right). \quad (16)$$

The Eddington limit depends only upon the mass of the star or black hole and applies to steady accretion. There are various ways by which super-Eddington luminosities can be obtained, but (15) is a useful guideline for the maximum luminosity which can be liberated in the steady state.

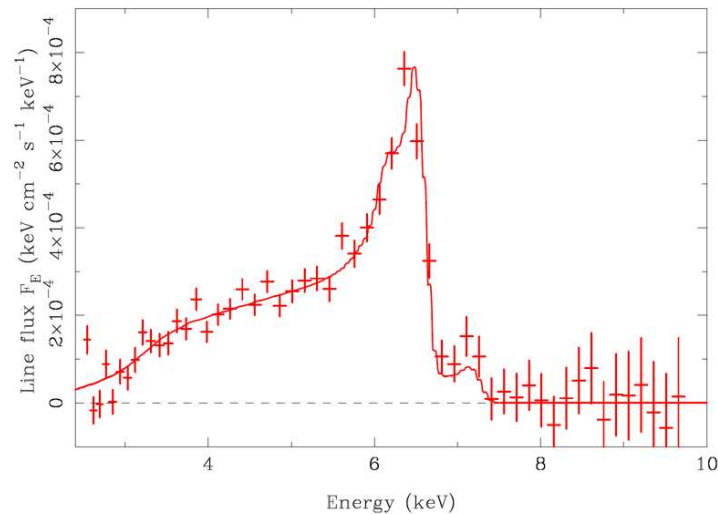
Accretion Discs

It is most unlikely that the matter has zero angular momentum, because of random gravitational perturbations acting on the infalling matter. The matter then collapses along the angular momentum axis of the infalling material. In the case of a black hole, a disc forms about the black hole and extends in to the last stable orbit. To do this, the matter must transfer its angular momentum outwards through the disc through the action of viscous forces, which at the same time results the material of the disc is heated by the viscous forces.

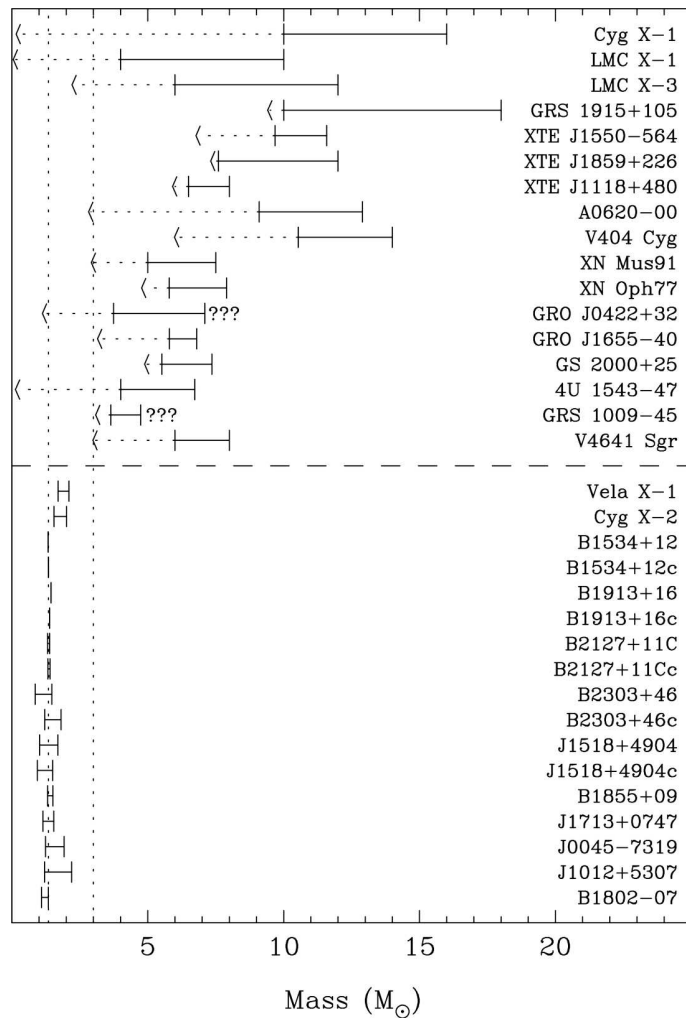
There is convincing evidence from spectral observations with the Newton-XMM X-ray observatory for the presence of asymmetric fluorescent $K\alpha$ emission at 6.4 keV in their spectra. The line is broadened on its low energy wing. The effect has been observed with reasonable signal-to-noise ratio in the spectrum of the Seyfert galaxy MCG-6-30-15.

Accretion Discs

The redshift of the line extends to about 4.5 keV. The preferred model to account for this large redshift is that it is associated with the combined gravitational and transverse Doppler shifts associated with matter close to the last stable orbit about the black hole. For a Schwarzschild black hole, the rotational speed of matter at the last stable orbit is $c/2$ and that the maximum combined gravitational plus Doppler shift is $\nu_{\text{obs}} = \nu/\sqrt{2}$. If this interpretation is correct, it is of the greatest importance since it would mean that we can observe matter very close to the last stable orbit about the black hole and so have the opportunity to study the behaviour of matter in strong gravitational fields.

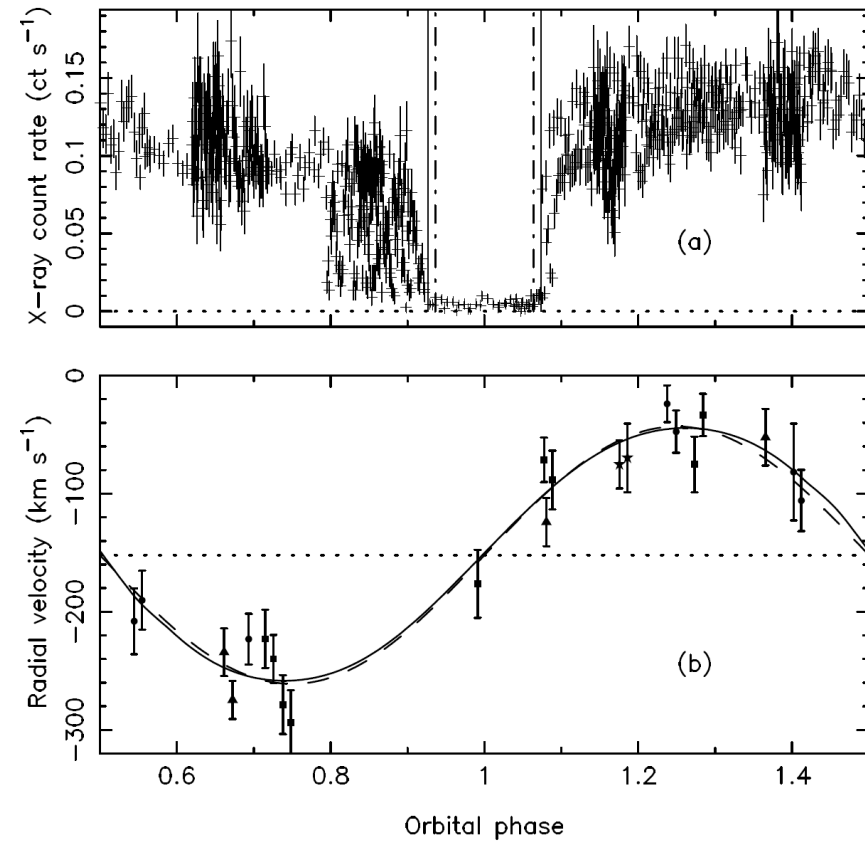
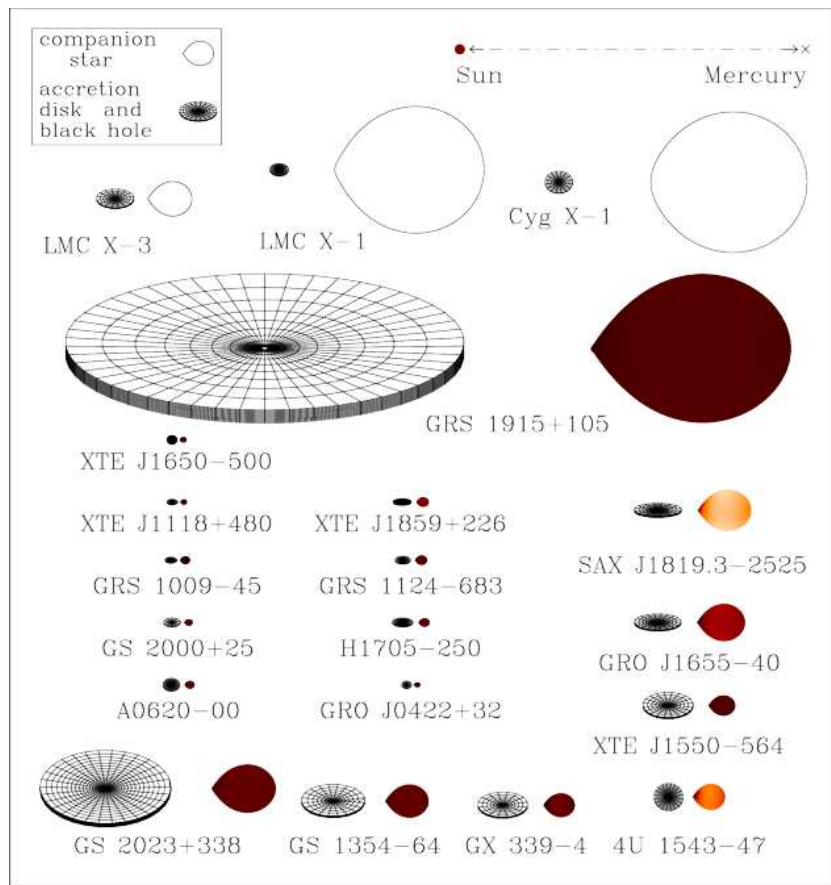


The Masses of Black Holes in X-ray binaries



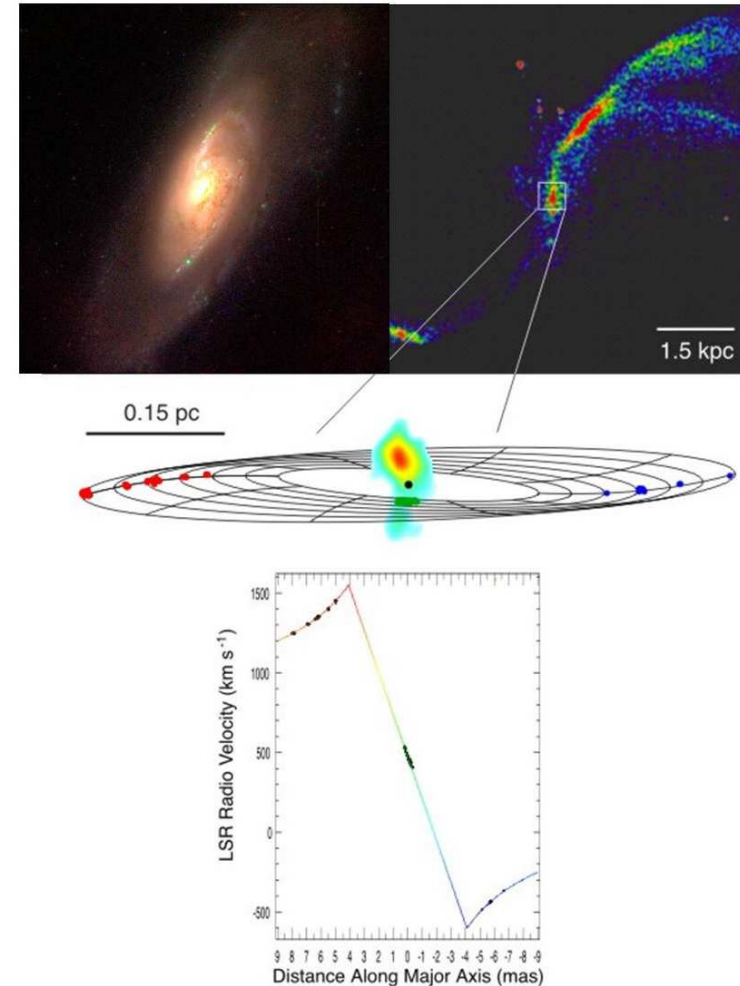
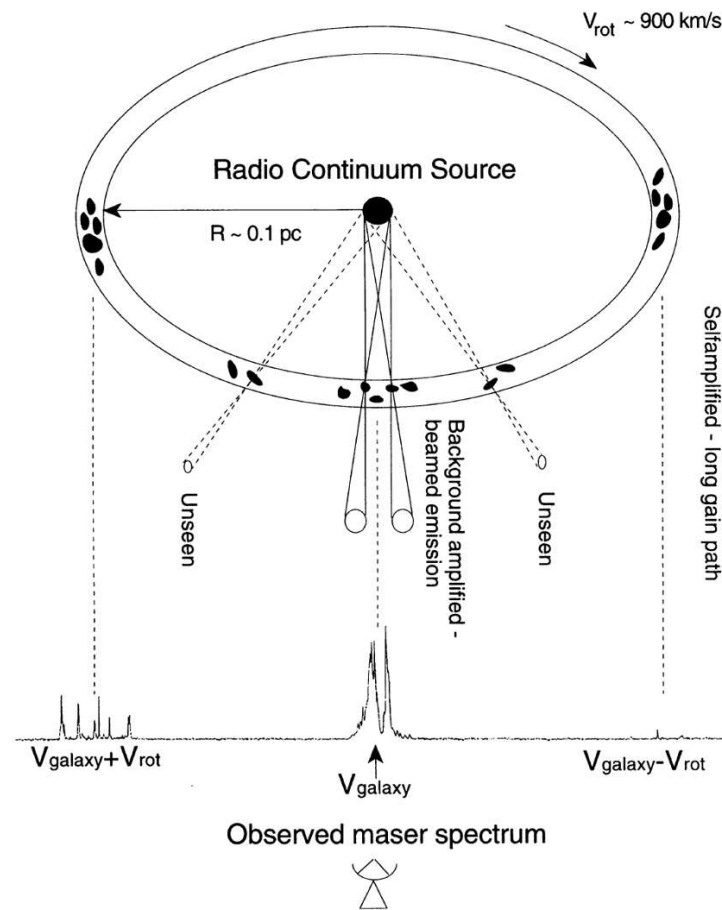
The methods of classical astrometry can be used to estimate the masses of the invisible compact objects which are the source of the intense X-rays observed in X-ray binary systems. In those systems in which the compact companion is a rapidly rotating neutron star, their masses always turn out to be about $1.4 M_{\odot}$. In cases in which there is no evidence for a neutron star, the masses of the unseen objects are significantly greater than $3 M_{\odot}$, indicating that the objects must be stellar mass black holes. In some cases, the compact object has mass about $10 M_{\odot}$.

Examples of Stellar Mass Black Holes



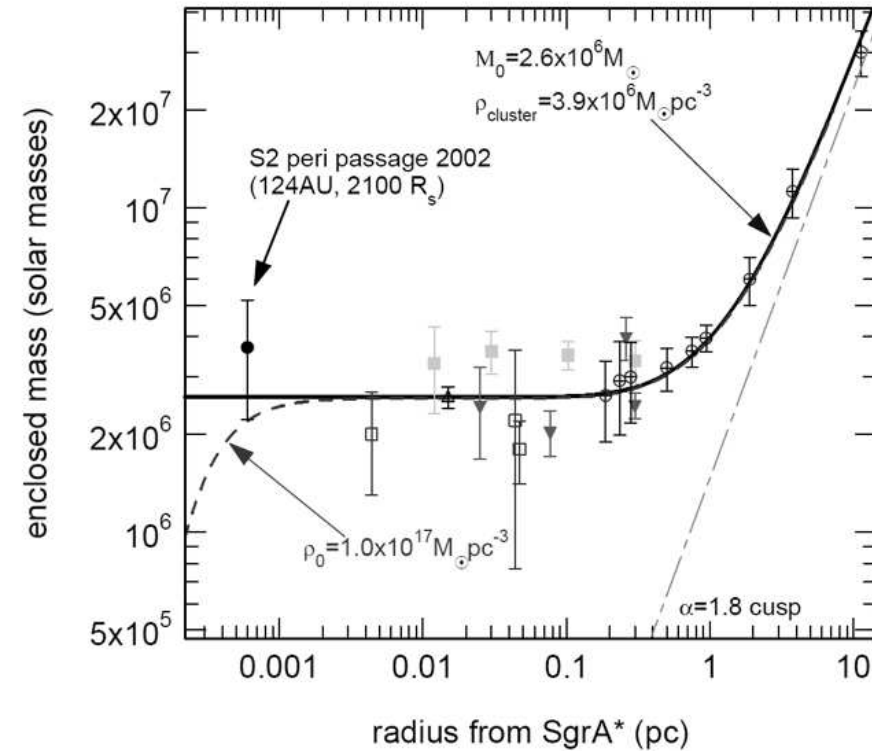
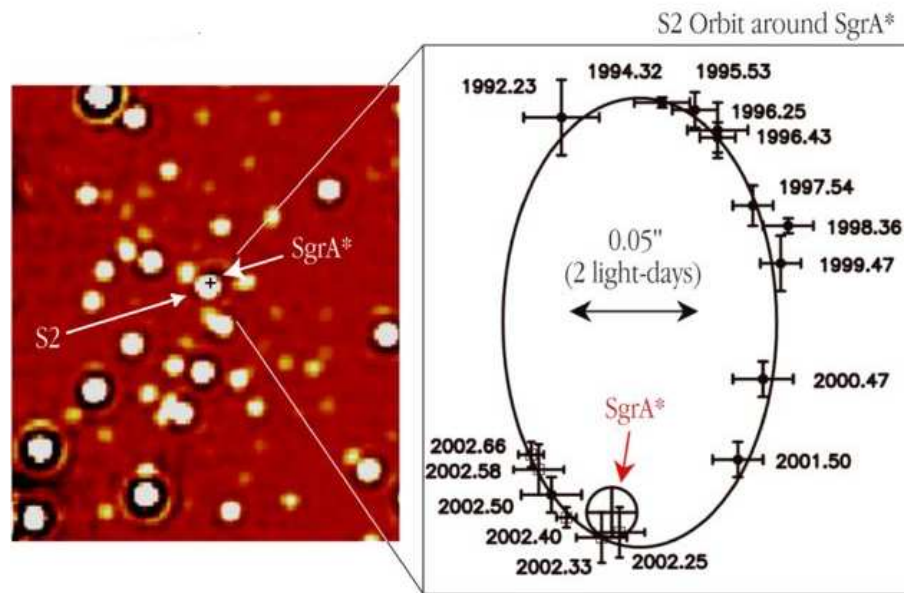
The X-ray binary M33 X-7 is an eclipsing binary and the primary star is a $70 \pm 6.9 M_{\odot}$ O star. The mass estimate of the black holes is $15.65 \pm 1.45 M_{\odot}$.

Black Holes in Nuclei of Galaxies - NGC 4258



In the case of NGC4258, the rotational speeds of H₂O masers follow a Keplerian relation as far in as they can be measured. The mass of the black hole is $3.7 \times 10^7 M_{\odot}$.

Black Holes in Nuclei of Galaxies - Galactic Centre



In the case of the Galactic Centre, Genzel and his colleagues observed the motions of infrared stars and determined precisely the mass of the central black hole. The mass of the black hole is $2.6 \times 10^6 M_\odot$.

Mass densities in the nuclei of galaxies

A summary of the masses and mass densities found in the nuclei of selected galaxies are listed below.

Galaxy	Mass of Nucleus (M_{\odot})	Mass Density ($M_{\odot} \text{ pc}^{-3}$)
NGC 4258	3.6×10^7	$\geq 4 \times 10^9$
M87	10^9	$\geq 10^6$
NGC3115	10^6	$\geq 10^8$
Galactic Centre	2.6×10^6	$\geq 10^{17}$
Globular Cluster	10^6	$\leq 10^5$

In NGC 4258, the mass density is at least 40,000 times greater than that of the densest globular clusters in our Galaxy. If the mass consisted of stars, the separation between them would be only about 100 AU and their collision times less than 10^8 years. Similar arguments can be made about the nature of the object present in the centre of our Galaxy – it is wholly convincing that there is a black hole with mass about $2.6 \times 10^6 M_{\odot}$ lurking in the centre of our Galaxy.

Clusters of Galaxies

Clusters of galaxies are the largest gravitationally-bound systems in the Universe and are often the seat of high-energy astrophysical activity. The hot intergalactic gas within clusters of galaxies enables the mass of the cluster and the gaseous environment to be determined in some detail. The equation of hydrostatic support for the intergalactic gas in a cluster of galaxies is

$$\frac{dp}{dr} = -\frac{GM(\leq r)\rho}{r^2}. \quad (17)$$

The pressure is related to the local gas density ρ through the equation of state $p = \rho kT / \mu m_H$ where m_H is the mass of the hydrogen atom and μ is the mean molecular weight of the gas. Differentiating the equation of state with respect to r and substituting into (16), we find

$$M(< r) = -\frac{kTr^2}{G\mu m_H} \left[\frac{d(\log \rho)}{dr} + \frac{d(\log T)}{dr} \right]. \quad (18)$$

Thus, the mass distribution within the cluster can be determined if the variation of the gas density and temperature with radius are known. The bremsstrahlung spectrum of the intracluster gas can be used to determine both its temperature and density distribution. In some clusters, the gas is dense enough to cool over cosmological time-scales resulting in *cooling flows*.

Mass distribution in clusters of galaxies

The hot gas acts as a tracer of the *total gravitating mass* in the cluster, including the dark matter which defines the gravitational potential. The typical total masses of rich clusters lie in the range 5×10^{14} to $5 \times 10^{15} M_{\odot}$, of which about 5% is attributable to the mass contained in the visible parts of galaxies and about 10 to 30% to hot intracluster gas. The remaining 60 to 85% of the mass is in some form of dark matter. Typically, the iron abundance of the hot gas is between about 20 and 50% of the solar value, indicating that the intergalactic gas has been enriched by the products of stellar nucleosynthesis.

The Chandra observations show that, while some clusters such as the Coma cluster can be well approximated by smooth X-ray profiles, other well-studied clusters display considerable structure in their X-ray distributions. Some of these are certainly due to the presence of powerful radio sources in the clusters. Presumably these events compress the gas allowing it to radiate with greater intensity. These considerations lead another characteristic of active galactic nuclei, the presence of jets.

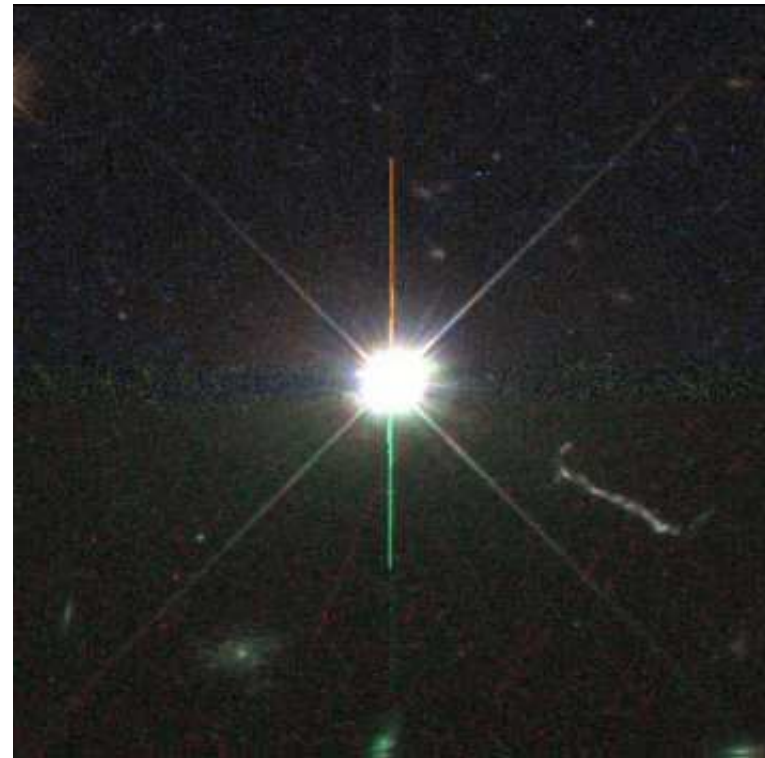
Jets

One of the remarkable phenomena which seem to accompany most manifestations of high energy astrophysical processes associated with compact objects is the presence of highly collimated jets of relativistic material. The best known of these are those associated with extragalactic radio sources and objects such as M87 and 3C273.

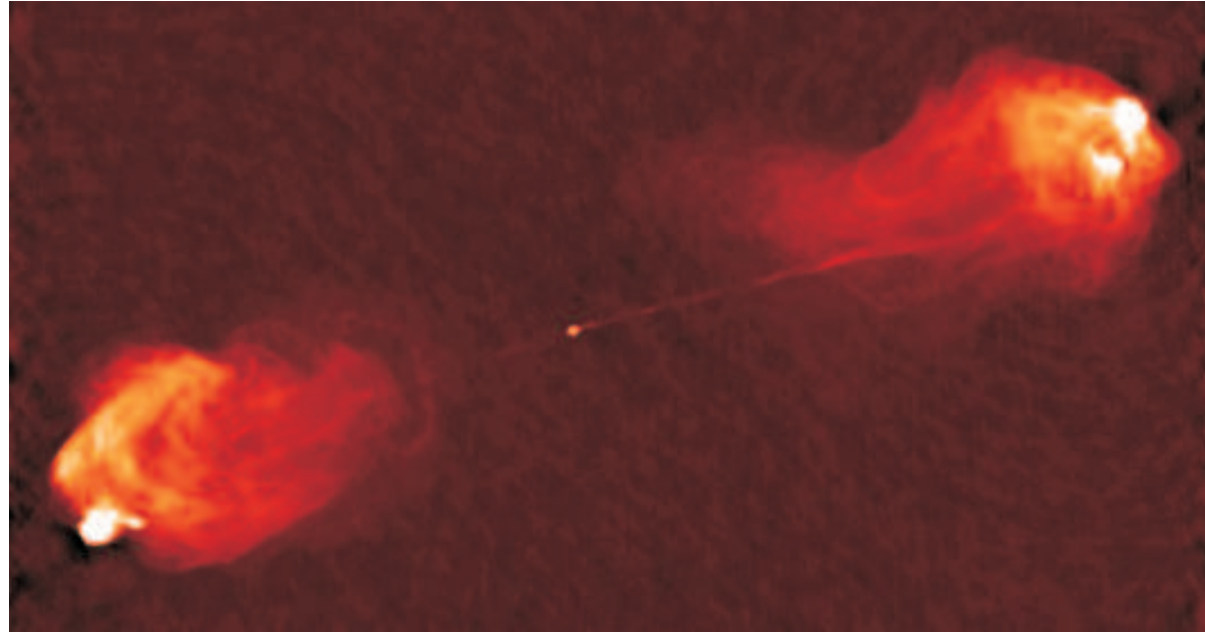
M87



3C 273

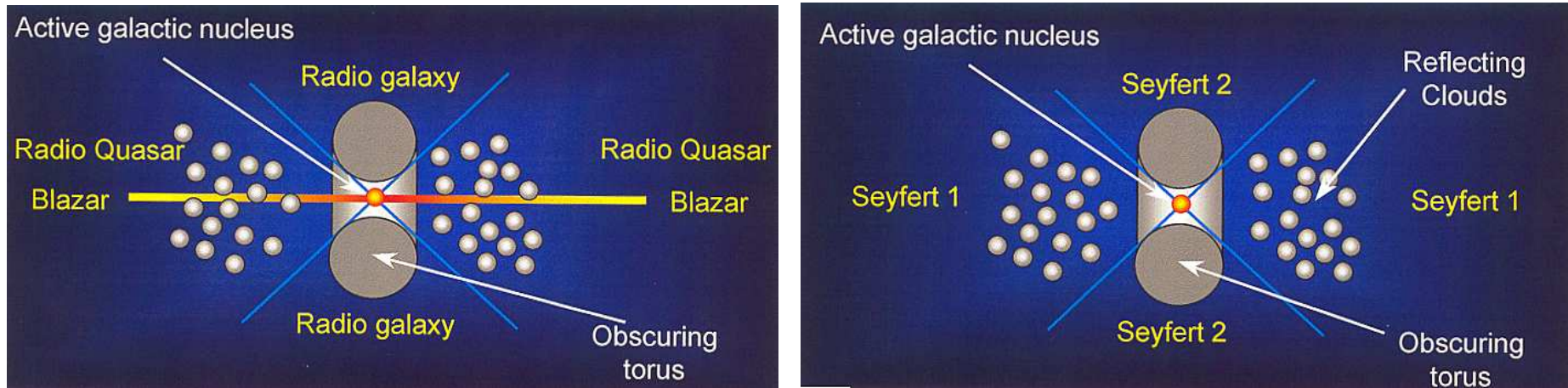


Cygnus A



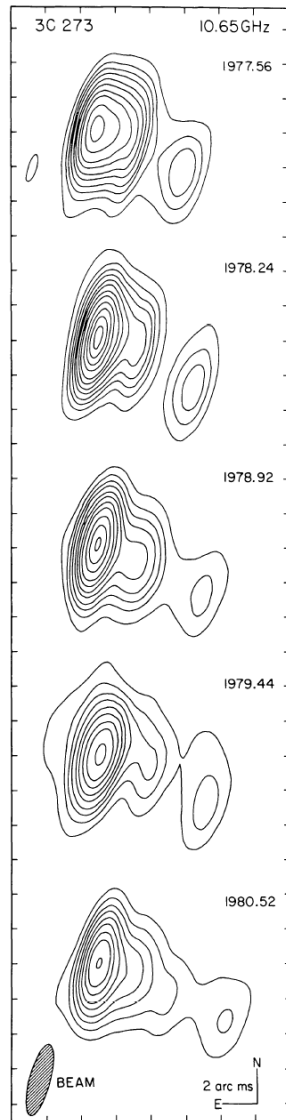
The most common examples of relativistic jets are found in the extragalactic radio sources. In sources such as Cygnus A, highly collimated jets of relativistic particles emerge from the nucleus of the galaxy in opposite directions and inflate huge radio emitting cocoons. The locations at which the jets encounter the surrounding interstellar and intergalactic gas result in 'hot-spots' where particle acceleration takes place. These particles inflate the cocoon as the jet continues to penetrate the surrounding medium. The material of the jet must travel at speeds close to the speed of light and the hot-spots themselves advance through the surrounding medium at speeds up to about 0.1 or 0.2 c .

Unifications schemes



The radio galaxies and radio quasars found in complete samples are in remarkable agreement with orientation-based *unification schemes*. If there is an obscuring torus about the active nucleus, the quasar-like activity in the nucleus is only observed if the observer lies within a certain angle with respect to the axis of the torus. This scheme can account for the properties of the radio galaxies and radio quasars found in, for example, the 3CR sample of radio sources if the opening angle of the torus is about 45° . Similar schemes can account for the differences between the Seyfert I and Seyfert II galaxies – in the former, the nuclear regions are observed directly, whereas in the latter, these regions can only be observed in the reflected light of clouds well outside the region of the torus.

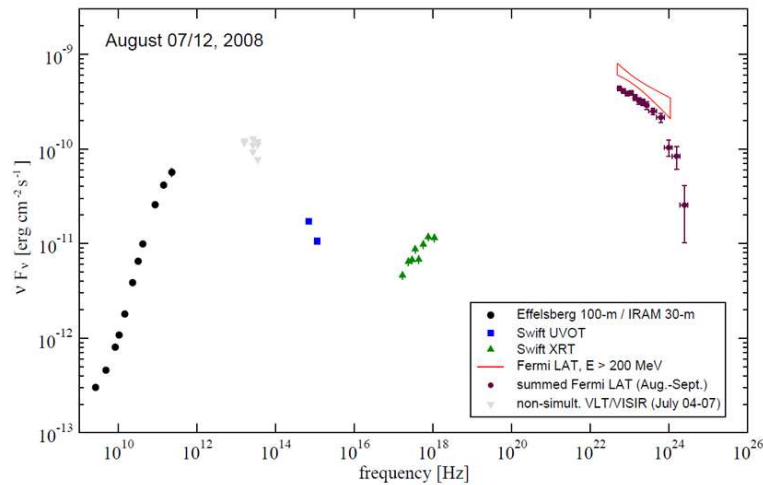
Superluminal velocities



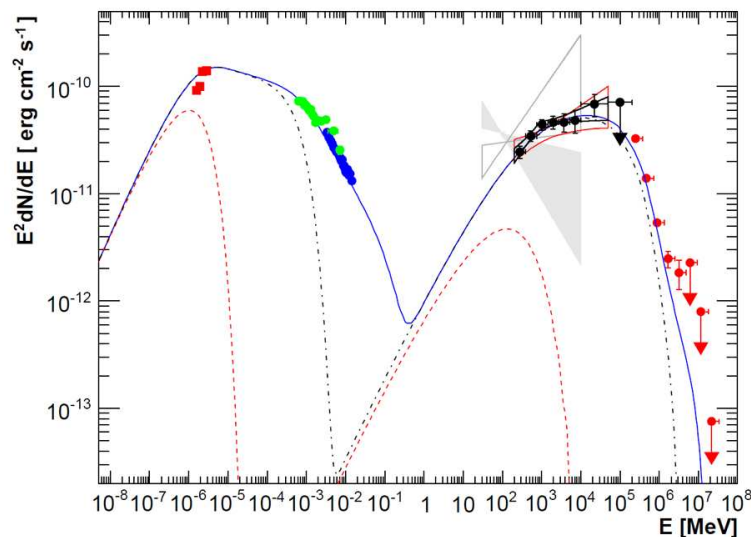
One of the big surprises of the study of luminous compact radio sources was the discovery of superluminal motions in sources such as 3C273 and 3C120. In 3C273, the jets are observed to move out from the nucleus at speeds up to 8 to 10 times the speed of light. This phenomenon has been found in many of the compact radio sources found in high frequency surveys. In the favoured relativistic ballistic model, it is assumed that this is an optical illusion associated with the fact that the jet is approaching the observer at a speed close to the speed of light at an angle close to the line of sight. In large samples of sources, superluminal speeds up to 35 times the speed of light are observed.

γ -ray active galactic nuclei

3C454.3

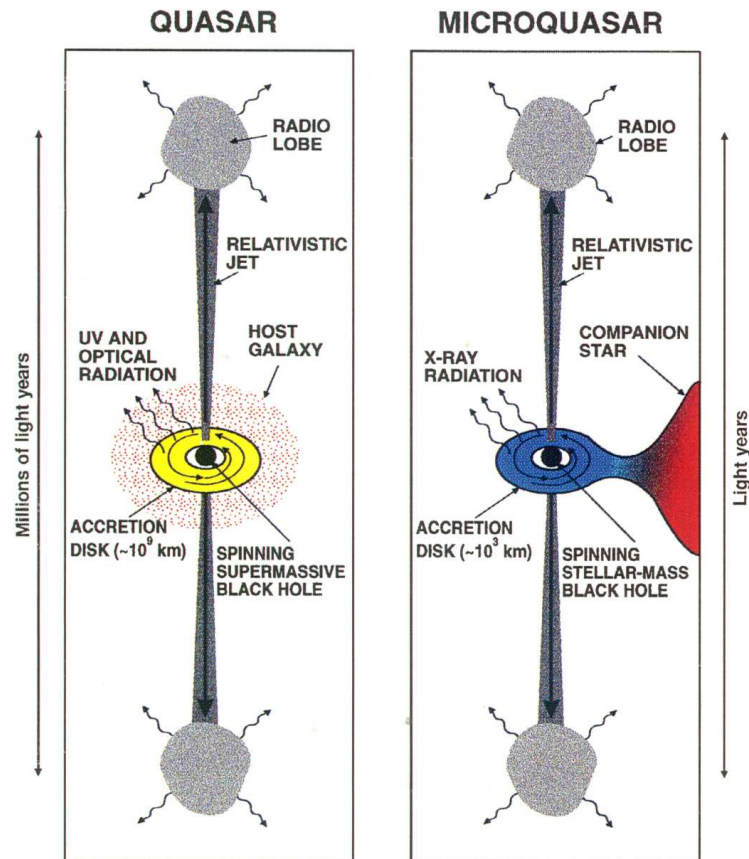


PKS2155-304



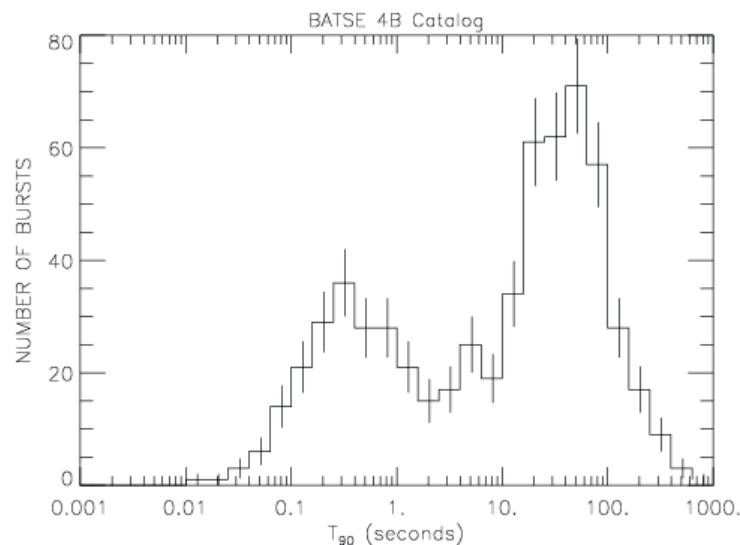
Further evidence for relativistic beaming has been found in the extreme γ -ray luminosities of the quasars detected by the Compton Gamma-Ray Observatory and by ground-based Cherenkov Arrays such as HESS. These are so extreme in luminosity and variability, that the effects of photon-photon scattering would destroy the γ -ray photons within the source region. The majority of these extreme γ -ray sources are also associated with objects which exhibit superluminal motion of their radio source components. The natural explanation for these enormous luminosities is that they are boosted by the same type of relativistic beaming which is responsible for the observation of superluminal motions.

Microquasars



In 1994 Mirabel and Rodriguez discovered that one of the Galactic X-ray binary source GRS 1915+105, which contains a stellar mass black hole, exhibits superluminal motion. They demonstrated convincingly that this class of source provides more or less exact counterparts for the phenomena observed in radio galaxies and radio quasars, but scaled down by a factor of about one million - they named these objects *microquasars*. Both the luminosity and the time-scale of variability of the sources are proportional to the mass of the black hole. The scaling down by a factor of one million means that phenomena, which would only be observable over periods of decades, or centuries, in the extragalactic case can be observed within minutes or hours.

γ -ray bursts



The last example of sources in which relativistic beaming must play an important role are the γ -ray bursts. It is now certain that these objects lie at cosmological distances and are the most luminous objects in the Universe for the seconds or minutes during which the burst lasts. To account for the luminosities and short duration of the bursts, relativistic motions are again invoked, this time in the form of a relativistic blast wave resulting from a catastrophic event, probably associated with the collapse of the core of a massive star, or possibly with the coalescence of a binary neutron star system.